ground water

Modeling Time Series of Ground Water Head Fluctuations Subjected to Multiple Stresses

by Jos R. von Asmuth[1,2], Kees Maas[1,2], Mark Bakker[1,2], and Jörg Petersen[3]

Abstract

The methods behind the predefined impulse response function in continuous time (PIRFICT) time series model are extended to cover more complex situations where multiple stresses influence ground water head fluctuations simultaneously. In comparison to autoregressive moving average (ARMA) time series models, the PIRFICT model is optimized for use on hydrologic problems. The objective of the paper is twofold. First, an approach is presented for handling multiple stresses in the model. Each stress has a specific parametric impulse response function. Appropriate impulse response functions for other stresses than precipitation are derived from analytical solutions of elementary hydrogeological problems. Furthermore, different stresses do not need to be connected in parallel in the model, as is the standard procedure in ARMA models. Second, general procedures are presented for modeling and interpretation of the results. The multiple-input PIRFICT model is applied to two real cases. In the first one, it is shown that this model can effectively decompose series of ground water head fluctuations into partial series, each representing the influence of an individual stress. The second application handles multiple observation wells. It is shown that elementary physical knowledge and the spatial coherence in the results of multiple wells in an area may be used to interpret and check the plausibility of the results. The methods presented can be used regardless of the hydrogeological setting. They are implemented in a computer package named Menyanthes (www.menyanthes.nl).

Introduction

Transfer function noise (TFN) models are a convenient tool for modeling the evolution of a wide range of variables. The general theory of time series analysis (Box and Jenkins 1970) originally stems from the statistical sciences. Because of their statistical background, the so-called autoregressive moving average (ARMA) time series models can be applied to all sorts of data, as long as the behavior of the system to be modeled is sufficiently linear or can be linearized by transforming the data. Time series models are especially useful for modeling systems whose behavior cannot, or not easily, be described in terms of physical laws and properties (e.g., economical data). In addition, TFN models are often used in hydrology and other sciences because they are relatively easy to construct and at the same time they can yield very accurate predictions.

When an ARMA type TFN model is applied to a data set, the so-called model order has to be specified. The model order includes the number of autoregressive and moving average parameters in both the deterministic and stochastic parts of the model and the delay time of the transfer function. Box and Jenkins devised an iterative model identification procedure to guide the modeler in finding the optimal model order. First, an initial model order is chosen based on statistical criteria like the cross-correlation function between the explained and explanatory variables. Second, the parameters of the model are estimated by minimizing the variance of the "innovations" or one-step-ahead prediction error using an optimization

[1]Corresponding author: Water Resources Section, Faculty of Civil Engineering and Geosciences, Delft University of Technology, P.O. Box 5048, 2600 GA, Delft, The Netherlands; +31-30-6069512; fax +31-30-6061165; jos.von.asmuth@kiwa.nl

[2]Kiwa Water Research, Department of Water Systems Management, P.O. Box 1072, 3430 BB, Nieuwegein, The Netherlands.

[3]Nature-Consult, Hackelbrink 21, D-31139, Hildesheim, Germany.

Received April 2007, accepted August 2007.

doi: 10.1111/j.1745-6584.2007.00382.x

algorithm. Third, the adequacy of the model is checked diagnostically using statistical criteria like the auto- and cross-correlation functions of the innovations. If the model does not yet meet the criteria, the model order is updated and the procedure is repeated until the modeler finds the results satisfactory. A disadvantage of this approach is that the results of the model identification procedure can be ambiguous (Hipel and McLeod 1994) and the process itself is rather heuristic and can be knowledge and labor intensive (De Gooijer et al. 1985).

Von Asmuth et al. (2002) presented the principles of a new type of TFN model that is optimized for use on hydrologic problems and operates in a continuous time domain. In this approach, the discrete transfer function used in ARMA models is replaced by a simple analytical expression that defines the impulse response function. The resulting class of models is referred to as predefined impulse response function in continuous time (PIRFICT). Von Asmuth et al. (2002) showed that PIRFICT models overcome a series of limitations of ARMA TFN models, including the use of irregular or high-frequency data and the modeling of systems with a long memory. In addition, application of the PIRFICT model does not require a Box-Jenkins style model identification procedure. Since the transfer functions are confined a priori to physically plausible behavior, there is no need to identify the "order" of the transfer functions on statistical grounds. Therefore, application of the model is standardized, which facilitates implementation in a computer package such as Menyanthes (www.menyanthes.nl). When the PIRFICT method was introduced (Von Asmuth et al. 2002), we restricted ourselves to the case of a single input/output series. Here, we will extend the method to cover more complex, real world situations where multiple stresses influence head fluctuations at one or multiple observation wells simultaneously.

Two important aspects of dealing with complex data sets are addressed in this paper. The first one is the treatment of different types of stresses within the model. Different stresses require different parametric impulse response functions. Von Asmuth et al. (2002) used the Pearson type III function for modeling the effect of precipitation surplus. Here, we will introduce analytical solutions of elementary hydrogeological schematizations as guides to develop appropriate impulse response functions for other stresses. We will also show that from a physical point of view, different stresses do not always have to be connected in parallel and get a separate transfer function, as is the standard procedure in ARMA TFN modeling. The second aspect deals with the interpretation and checking of the plausibility of the results. While the time series literature commonly involves the analysis of individual time series, using the PIRFICT approach, one can analyze and process all available series of heads in an area in batch. Given that they are part of the same hydrological system, the results of neighboring observation wells may show a spatial coherence, which yields valuable extra information as regards the properties of the system and the plausibility of the results. In this paper, however, all series are still modeled separately and the resulting spatial patterns are analyzed a posteriori. Future research will include methods to impose spatial coherences a priori in the model.

This paper is organized as follows. First, we discuss how different types of stresses are dealt within the model. We illustrate the approach by analyzing a single series being influenced by precipitation, evaporation, ground water withdrawal, and river-level fluctuations. Second, results are presented for a case where data are available from multiple observation wells. A discussion and conclusions are given at the end of the paper.

Methodology

From a Single to a Multiple Input Model

The basic equation of an ARMA model, which is discrete in time, is equivalent to the following convolution integral in continuous time (Von Asmuth et al. 2002):

$$h_i(t) = \int_{-\infty}^{t} R_i(\tau)\theta_i(t-\tau)\mathrm{d}\tau \qquad (1)$$

where h_i [L] is the predicted head at time t attributable to stress i. R_i is the value of stress i at time t, and θ_i is the transfer or impulse response function of stress i. In ARMA time series models, multiple stresses are dealt with by connecting them in parallel and assigning a separate transfer function to each. The output series is then obtained by summing the separate effects of all stresses. For the case where a number of N stresses influence the head, the equations of a continuous time TFN model may be written as follows:

$$h(t) = \sum_{i=1}^{N} h_i(t) + d + n(t) \qquad (2)$$

where h is the observed head at time t, d is the local drainage level relative to some reference level [L], and n is the residual series [L].

Several main types of stresses can be distinguished. These types include precipitation (p), evaporation (e), ground water withdrawal (or injection) (w), surface water level (s), barometric pressure (b), and (hydrological) interventions (m). Please note that tidal fluctuations, on whose effect a large volume of paper is devoted, are included in the s type. From a physical point of view, a ground water system is likely to respond to different types of stresses differently, but there are also certain stresses that will cause a very similar response. In the latter case, separate stresses do not necessarily need separate response functions. For instance, the effect of evaporation e on the head h is essentially the same as that of precipitation p, but it is negative, and may be modeled as follows:

$$h_e(t) = \int_{-\infty}^{t} -e(\tau)f\theta_p(t-\tau)\mathrm{d}\tau \qquad (3)$$

where θ_p is the response of the system to precipitation and f is a reduction of e as compared to the reference

evaporation series. The evaporation factor f is a parameter that depends on soil and land cover and should not be confused with the crop factor (e.g., Penman 1948), as the latter is used for a crop that is optimally supplied with water, while f also incorporates the average reduction of the evaporation due to actual soil water shortages. For sake of simplicity, we consider f to be constant. Although it may actually be a function of time, the use of an average reduction factor is in fact already an improvement upon traditional ARMA modeling practice, where f is often simply ignored. In the case of the barometric pressure b, which codetermines the loading on a (semi)-confined aquifer, we propose to use the time derivative in the convolution:

$$h_b(t) = -\int_{-\infty}^{t} \frac{\mathrm{d}b(\tau)}{\mathrm{d}\tau}\theta_b(t-\tau)\mathrm{d}\tau \tag{4}$$

in order to be able to use an impulse response function θ_b that behaves similar to the other stresses, as a step change of b will result in a quick increase of h, followed by a slow decay whenever the aquifer is not completely confined.

Interventions are defined as structural changes to a hydrologic system, like forest clearing, construction of ditches or drainage systems, and so on. In general, the nature of an intervention determines the manner in which it should be modeled. For example, if the intervention causes a sudden change in actual evaporation on time t_m, such as a forest clearing, it may be modeled as follows:

$$h_m(t) = \int_{-\infty}^{t} m(\tau)k\theta_p(t-\tau)\mathrm{d}\tau \tag{5}$$

where $m(t) = 0$ for $t < t_m$ and $m(t) = 1$ for $t > t_m$, and k is a parameter representing the change caused by the intervention. Another example is a change in the level of a floodgate. This intervention itself acts as an independent stress on the system, and, in such cases, a new response function θ_p should be estimated. It is noted that it is possible that the hydrogeological properties of the system are changed significantly by an intervention. In that case, the response of the system to all stresses is changed and Equation 1 becomes:

$$h_i(t) = \int_{-\infty}^{t_m} R_i(\tau)\theta_{i_1}(t-\tau)\mathrm{d}\tau + \int_{t_m+\Delta t}^{t} R_i(\tau)\theta_{i_2}(t-\tau)\mathrm{d}\tau \tag{6}$$

where θ_{i1} and θ_{i2} are the response functions before and after the intervention, respectively. A transition period of Δt, during which the system shifts from one state to another, should be omitted from the data. The length of this period depends on the response time of the system.

The Impulse Response Functions for Different Types of Stresses

Under a wide variety of hydrogeological settings, the response of an impulse of precipitation surplus may be simulated accurately with a Pearson type III distribution function (PIII) (Von Asmuth et al. 2002):

$$\theta_p(t) = A\frac{a^n t^{n-1}\exp(-at)}{\Gamma(n)} \tag{7}$$

where A, a, and n are parameters that define the shape of θ_p. The choice of this impulse response function was based on physical arguments, and it was shown that the PIII function was (at least) as effective as an ARMA type transfer function of optimal order. Although the PIII function is very flexible, it proves to be less effective for non-distributed types of stress. For ground water withdrawals (stress type w) and surface water level fluctuations (type s), we propose to use response functions inspired on analytical solutions of simple hydrogeological schematizations. Notice that the crucial issue in selecting a parametric impulse response function is whether the range of shapes it can take is sufficient to approximate the true response of the system accurately. In this sense, our viewpoint is that of time series analysis, where the only assumptions regarding the transfer model are that the system is linear and that the "model order" is adequate. Here, we assume that the functions chosen can capture the essential behavior of the stress type regardless of the exact geohydrological setting. A systematic comparison of the performance of different impulse response functions for different types of stresses, however, falls beyond the scope of this paper and will be dealt with in an upcoming paper.

For withdrawals (stress type w), we choose the well formula of Hantush (1956) as a blueprint. The Hantush formula assumes a fully penetrating well in an aquifer of infinite extent, with transmissivity T [L] and storage coefficient S [−], covered by a storage-free aquitard with resistance c [T]. While a standard pumping test yields a step response function, here we are looking for an impulse response function, which is the derivative of the step response function with respect to time:

$$\theta_w(t) = -\frac{1}{4\pi Tt}\exp\left(-\frac{r^2S}{4Tt} - \frac{t}{cS}\right) \tag{8}$$

where r denotes the distance between the observation and the pumping well. Since we intend to use this formula in other hydrogeological settings as well, we convert this equation to the following parametric impulse response function:

$$\theta_w(t) = -\frac{\gamma}{t}\exp\left(-\frac{\alpha^2}{\beta^2 t} - \beta^2 t\right) \tag{9}$$

where α, β, and γ are just parameters that no longer have a transparent physical meaning (except for cases where Hantush assumptions happen to be satisfied). For surface water fluctuations (stress type s), we choose the so-called polder function of Bruggeman as a blueprint (Bruggeman 1999). This function represents a sudden unit increase of the water level at the boundary of a one-dimensional semi-confined aquifer of semi-infinite extent. The derivative gives the impulse response function θ_s, the response to a very short rise and fall of the surface water level:

$$\theta_s(t) = -\frac{1}{\sqrt{\frac{4\pi k D t^3}{x^2 S}}} \exp\left(-\frac{x^2 S}{4kDt} - \frac{t}{cS}\right) \qquad (10)$$

where x denotes the distance between the surface water feature and the observation well. We convert the physical parameters to the abstract parameters α', β', and a scaling factor γ', so that θ_s becomes:

$$\theta_s(t) = -\frac{\gamma'}{\sqrt{\pi \frac{\beta'^2}{\alpha'^2} t^3}} \exp\left(-\frac{\alpha'^2}{\beta'^2 t} - \beta'^2 t\right) \qquad (11)$$

For stress type b (the barometric pressure), we chose the PIII function, that is, the same impulse response function as used for precipitation and evaporation, because pressure is a distributed type of stress, too. The adequacy of a time series model based on these impulse response functions may be checked with the aid of the methods described and illustrated in the coming paragraphs. The practical usefulness of these impulse response functions has been demonstrated through application to thousands of wells in Europe, Australia, and North and South America.

Parameter Estimation

The first step in the parameter estimation process is the evaluation of the model equations using an initial estimate of the parameters, which will result in a time series of model errors or residual series. When modeling hydrological data, the value of a model residual at a certain time is often correlated with its value at earlier times, so residuals cannot simply be modeled as a set of independent Gaussian deviates. Here, the model residuals are modeled with a separate noise model, which is given by:

$$n(t) = \int_{-\infty}^{t} \phi(t - \tau) \mathrm{d}W(\tau) \qquad (12)$$

where ϕ is the noise impulse response function and W is a continuous white noise (Wiener) process [L]. This is equivalent to an AR(1) model embedded in a Kalman filter under the pure prediction scenario in discrete time, when the response function ϕ is exponential (Von Asmuth and Bierkens 2005). In that case, the one-step-ahead prediction error or innovation series v of the noise model may be obtained as follows:

$$v(t) = n(t) - n(t - \Delta t)\exp(-\alpha \Delta t) \qquad (13)$$

The noise model is important for the parameter estimation process and for dealing with irregularly spaced data, but also for prediction, forecasting, and stochastic simulation purposes. For further details, we refer to Von Asmuth and Bierkens (2005), as the parameter estimation process itself is not influenced by the fact that the transfer model contains multiple stresses.

General Modeling Procedure

The model identification procedure devised by Box and Jenkins (1970) is that, first, the model order is specified, second, the parameters are estimated, and third, the model results are checked. The adequacy of the model results may be checked with statistical criteria like the autocorrelation and cross-correlation functions of the innovation series v. The autocorrelation function indicates whether the white noise assumption holds, which is a prerequisite of the algorithms used for the estimation of the model parameters and their covariance; it also indicates whether the order of the noise model is adequate. The cross-correlation functions between the innovation series v and the different input series indicate whether there are patterns left in the innovation series that could be explained by the input series. This gives an indication of the adequacy of the order of the transfer functions but also of possible nonlinearity in the relationships. If the model does not meet these so-called diagnostic checks, the model order is updated. This procedure is repeated until the optimal model order is identified (Box and Jenkins 1970).

As stated earlier, there is no need for identifying the order of the transfer model on statistical grounds in the PIRFICT approach, as the impulse response functions are chosen on physical grounds and span a whole range of ARMA model orders (Von Asmuth et al. 2002). In both cases, however, the modeler also has to identify the stresses that influence the ground water dynamics, decide which stresses to use, and check the results. Stresses that are not incorporated in the model can lead to erroneous results when their dynamical behavior is correlated with one or more of the other (already considered) stresses. On the other hand, the model may have difficulty in uniquely identifying all influences when there is a high number of stresses, a lack of pronounced dynamics of the stresses, or a low quality or scarcity of the data. The diagnostic checks introduced by Box and Jenkins are devised to assess whether the TFN model is adequate and optimal in a statistical sense, which remains important especially for the noise model, but does not exclude the possibility that the model results are influenced by noncausal correlations. Here, we propose the use of plausibility checks to guide the modeler in assessing whether the results of the transfer model are physically realistic. The resulting modeling procedure is illustrated in Figure 1.

The plausibility checks include the model residuals, the evaporation factor f, the local drainage base d, and the moments of the impulse response functions and their standard deviations. The model residuals, uniting all factors that are not accounted for by the model, are an important aid in identifying possible unknown stresses that may be a source of model distortions. Nonrandom patterns of the residuals in space or time reveal the fact that there are still stresses missing in the model. The patterns themselves often give enough information to pinpoint the nature and location of the missing stresses. The evaporation factor f is important, as the seasonal cycle in the evaporation is often present in other natural or anthropogenic stresses such as ground water withdrawals for agricultural or drinking water purposes as well. Regarding the drainage base, an estimate that is too low or too high may be caused by the influence of stresses that are not incorporated in the model or that are not well

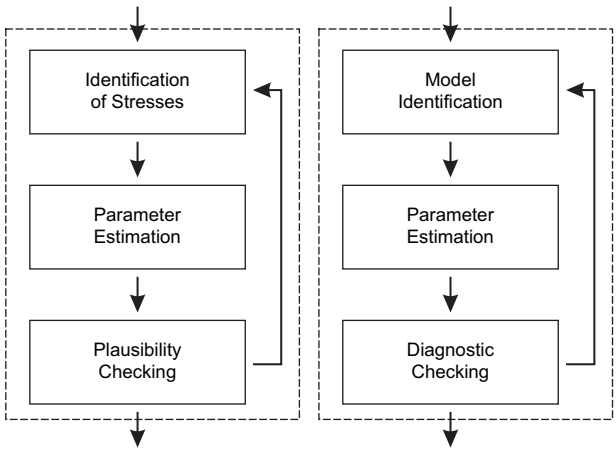

Figure 1. Proposed procedure for modeling time series of ground water heads in complex situations. The procedure for identifying the noise model is that of Box and Jenkins (1970). When both the plausibility and diagnostic checks are met, the results can be accepted for further use.

quantified. This can easily happen with stresses that do not show pronounced dynamics, such as more or less constant seepage or withdrawal rates. In addition, the moments of the impulse response functions of the different stresses provide relevant information. Moments can be used to characterize the functioning of the ground water system and can be related to its geohydrologic properties (Von Asmuth and Maas 2001; Von Asmuth and Knotters 2004). In contrast to physical parameters that are defined only in the context of a certain schematization, moments are related to common statistical terms and are more generally applicable. The j^{th} moment of an impulse response function is defined as follows:

$$M_j = \int_{-\infty}^{\infty} t^j \theta(t) \mathrm{d}t \tag{14}$$

where M_0 represents the area under the impulse response function, $\mu = M_1/M_0$ is the mean of the impulse response function, and $\sigma^2 = M_2/M_0 - \mu^2$ is the variance. Matching of moments is a common technique for solving differential equations, amongst others in transport modeling (e.g., Yu et al. 1999; Luo et al. 2006).

Example Applications

Single Head Series

The functioning and results of a multiple input PIRFICT model on a single well located in the northern part of the province of Limburg (the Netherlands) are presented in this subsection. The well, with the national code 46DP0032, has two screens. We consider only the top one, which is located 13 m below the surface. The well is located on the edge of the floodplain of the river Meuse in an aquifer that consists of coarse gravelly sands overlain by finer sands which originate from river deposits. In addition to the river-level fluctuations, the head is influenced by precipitation and evaporation and by a pumping station near the town of Bergen where ground water is withdrawn for drinking water production.

Time series data of all stresses are available. The precipitation and potential evaporation series originate from stations of the Royal Dutch Meteorological Institute in Venray and Eindhoven, respectively. The river levels were monitored at a dam in Sambeek, downstream of well 46DP0032; the pumping rates were obtained from the drinking water company of Limburg. The parameters of all three impulse response functions are optimized using the methods described in Von Asmuth and Bierkens (2005). Here, we will consider the results of the transfer part of the model and of this individual series only, after the first run of the model. The model results and parameter estimates are summarized in Table 1. In the table, two parameters are given that define the goodness of fit: the percentage of variance accounted for (R^2_{adj}) and the root mean squared error. In the definition of R^2_{adj}, the residual variance $\sigma^2_{n(t)}$ is weighed according to the variance $\sigma^2_{h(t)}$ of the original signal in the following manner:

$$R^2_{\text{adj}} = \frac{\sigma^2_{h(t)} - \sigma^2_{n(t)}}{\sigma^2_{h(t)}} \times 100\% \tag{15}$$

The results of the time series model are shown in Figure 2, where the measured heads h (dots) and predicted heads $\sum_{i=1}^{N} h_i + d$(solid) are plotted together in the upper graph, while h_i is plotted for every stress in the graphs beneath. Thus, the ground water level series is decomposed into four partial series, which show the effects of the individual stresses. For example, it may be observed that the recent series of wet years in the Netherlands (1999 to 2002) has led to an overall increase in the ground water levels. Furthermore, the effect of evaporation does not vary much from year to year but shows a distinct seasonal pattern as it is mainly influenced by temperature and solar radiation. The river level has little effect as it is maintained by dams, except for high-water events when the river leaves its channel and enters the floodplain. In those cases, the head responds very quickly and shows distinct peaks. Finally, heads show a gradual decline since 1994 due to the ground water withdrawal that started around that time. Note that these distinct differences in dynamic behavior allow the time series model to distinguish the effects of the individual stresses. Also note that the frequency of the ground water level observations changes around 1992 from four times a year to once a week. This does not pose a problem for the model, as the impulse response equations are continuous in time and predictions are not fixed to a certain time discretization.

For each of the different stresses, an impulse response function is estimated (although not always independent from the other stresses, see Equations 3 through 5). The impulse response function forms the heart of the time series model and represents the response of heads to a unit impulse of the stress. The shape of the impulse response function depends on the position of the observation well and the properties of the system. As an example, the impulse response function of the level of the river

Table 1
Model Results and Parameter Estimates for the Ground Water Head Series Observed in Well 46DP0032

Input series	Stress Type	Parameter	Value	σ
Venray	Precipitation	$A(M_{0,p})$	299.2	23
		b	0.003117	0.00033
		n	0.898	0.025
Eindhovenentry	Evaporation	f	1.16	0.076
P.S. Bergenentry	Pumping well	α	2.58	2.4
		β	0.0522	0.027
		γ	0.00585	0.03
		$M_{0,w}$	-3.63×10^{-5}	5.68×10^{-6}
SambeekBoven	River	α'	0.02527	0.094
		β'	0.0368	0.13
		γ'	0.7656	0.057
		$M_{0,s}$	0.7279	0.0939

Note: $R^2_{\text{adj}} = 92.0\%$. Root mean squared error = 0.068 m. Drainage base = 11.53 m.

Meuse is plotted in Figure 3. From the graph, one can infer that the heads indeed respond quickly to a rise and fall in river level, as the impulse response function (solid line) peaks in less than half a day. Apart from its dynamic response, one is often also interested in the stationary influence of a certain stress. This is represented by the step response function (dashed line), which is the integral of the impulse response function with respect to time; the step response represents the response of the system to a sudden and then ongoing rise of the river level. The level that the step response function approaches toward infinity is the zeroth moment (M_0), also known as the gain in the time series analysis literature. Using Equation 11, we can obtain M_0 for stresses of type s as follows:

$$M_{0,s} = \int_0^\infty \theta_s(t)\mathrm{d}t = \gamma' \exp(-2\alpha') \tag{16}$$

In the case presented, $M_{0,s}$ for the river Meuse is 0.73 m, which means that a river level rise of 1 m will eventually lead to a ground water level rise of 73 cm on this location. For as long as the assumption of linearity holds, the zeroth moment can be used for quick scenario calculations, as the multiplication of $M_{0,s}$ and a planned

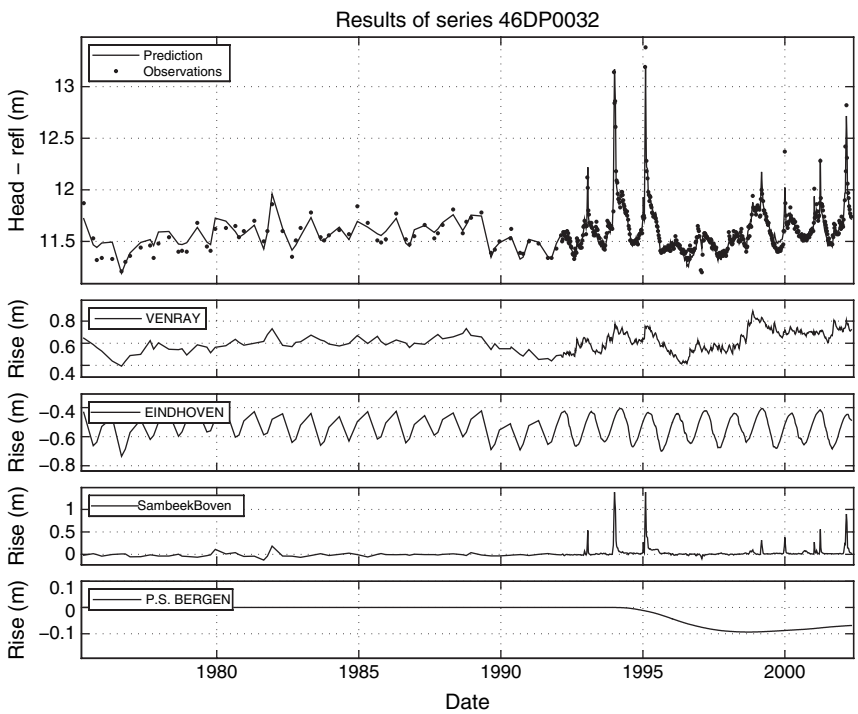

Figure 2. The ground water head fluctuations in well 46DP0032 (top) decomposed in four partial series due to (from top to bottom) rainfall, evaporation, river-level fluctuations, and a pumping station. Adding the partial series and the estimated drainage base *d* (Table 1) results in the predicted series.

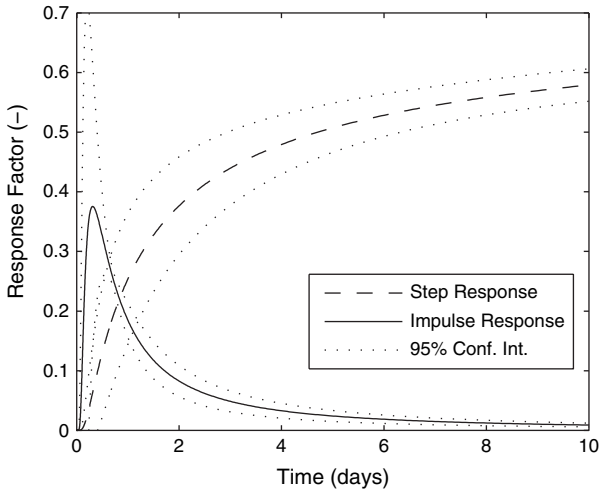

Figure 3. Estimated impulse and step response functions of observation well 46DP0032 for the level of the river Meuse (measured at dam Sambeek-Boven).

rise in the river level yields a prediction of the ground water level rise. Note that the standard deviation of $M_{0,s}$ is reasonable, whereas the standard deviation of parameter α' is large (a similar case is true for $M_{0,w}$ of the ground water withdrawal). This is caused by the covariance between the parameters.

Multiple Head Series

We will illustrate the procedure in which the results from multiple observation wells may be interpreted and checked in a second application. This application concerns a drinking water production area with multiple observation wells located in the northwestern part of Germany, in an area called "Harlingerland" near the Town of Esens. Ground water is withdrawn by the drinking water company Oldenburgisch-Ostfriesischer Wasserverband (OOWV) at a current rate of 9 million m^3/year. The 15 pumping wells are clustered in two rows, which are more or less placed in series (Figure 4). The well screens are located at a depth of 25 to 40 m from the soil surface. The withdrawal rate history (Figure 5) shows a marked increase in the period from 1972 until 1976. Such a rate change is very important for a reliable estimate of the influence of a pumping well, as it will have caused a marked drawdown. Furthermore, the withdrawal rates show a distinct seasonal cycle caused by factors like the increased watering of yards in dry periods. The withdrawal rate is obtained by summing the pumping rates of the individual wells. Data on the individual wells, which are controlled separately, are available only since 1992. Anyway, use of the individual pumping rates is not straightforward, as the number of 15 wells is too high to estimate their influence independently. Ground water dynamics are recorded at 116 observation wells with a total of 139 screens in a circle with a radius of 5 km around the pumping wells. The screens depths range from less than 1 to more than 90 m from the surface. Part of the wells are monitored every 2 weeks and the other part monthly. The period in which the wells were monitored differs from well to well, with the earliest measurements dating back to 1964, while other wells were installed as recently as 1999. In some of the wells, monitoring stopped in 1975, while in some others, the period between 1975 and 1998 is missing. The aquifer in the area consists mainly of sands; in some parts, a clay layer separates the phreatic from the deeper aquifer.

The head fluctuations are modeled with precipitation, reference evapotranspiration, and ground water withdrawals; there are no rivers or other important fluctuating surface water in the area. Results of the 139 time series models are summarized in Table 2, where the minimum, median, and maximum value of the parameters in all 139 models are given, along with their 95% confidence interval. The median value of R^2_{adj} points out that the fit of most models is good, although there are clearly outliers in the results, as the extremes of most parameter estimates are not within a range that is physically plausible. This does not mean that the estimates are necessarily biased, as most extremes are accompanied by large standard deviations. For these cases, a confidence interval of $\pm 2\sigma$ includes the value zero, but also a realistic value indicating that the quality or quantity of the data are not sufficient to determine the value of that parameter.

The only estimate in Table 2 that does seem biased is the minimum value for the evaporation factor f, which is

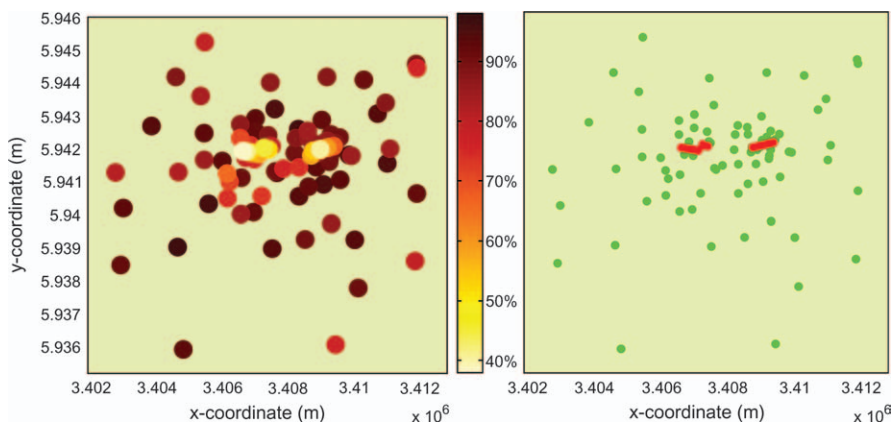

Figure 4. Spatial distribution of the percentage of variance accounted for (R^2_{adj}), in plan view (left figure). Low values for R^2_{adj} are found near the 15 pumping well screens that are clustered in two rows (red dots in right figure).

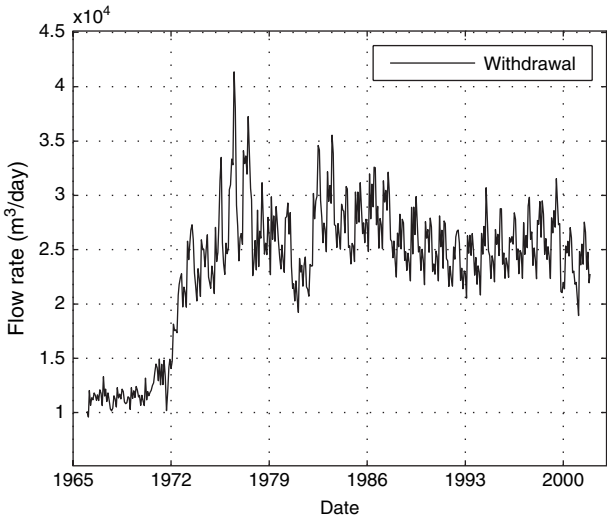

Figure 5. Ground water withdrawal history at location Harlingerland. The flow rate is obtained by summing the rates of the individual pumping wells.

very low (upper 95% limit is 0.4). In this case, however, the zeroth moment of the evaporation $M_{0,e}$ which is defined as follows:

$$M_{0,e} = \int_0^\infty f\theta_p(t)\mathrm{d}t = fA \tag{17}$$

does have a large confidence interval (± 941), as the influence of precipitation itself (A) cannot be determined from the data accurately (the probable cause is that the period in which data are available for this particular series spans only 16 months, with one observation per month).

To determine the reason for the lower R^2_{adj} of some models, its spatial distribution is plotted (Figure 4). From the figure, it is clear that the model fits are lowest in the immediate vicinity of the pumping wells. This suggests that the influence of the individual wells is not modeled correctly, which is indeed the case, as the withdrawal rate of the total wellfield is incorporated in the model, not the rates of the individual wells. The individual model fits (Figure 6) give the same indication. Near the wellfield, the head fluctuates wildly when the individual pumping wells are shut on and off. The predictions, however, follow only the general drawdown pattern. At some distance, the predictions fit the head fluctuations much better.

The model fit is also lower in some of the shallower wells. The head series in those cases show distinct signs of (threshold) nonlinearity (e.g., Knotters and De Gooijer 1999). The PIRFICT method can currently handle threshold nonlinearity for precipitation and evaporation, but not yet for other stresses, so this was not considered further at this time.

Next, we focus on the estimated influence of the wellfield, which was an important objective for doing the time series analysis of this site. Using Equation 9, we find that the zeroth moment of a well is given by (Hantush 1956):

$$M_{0,w} = \int_0^\infty \theta_w(t)\mathrm{d}t = -2\gamma K_0(2\alpha) \tag{18}$$

in which K_0 is the modified Bessel function of the second kind and zeroth order (Abramowitz and Stegun 1964). First, we remove all wells with estimates of $M_{0,w}$ with large confidence intervals, as they are of little value and only blur our view on the other results; we choose a cutoff value of 8×10^5. The 34 series that were disregarded all lack the period from 1972 to 1976 in which the withdrawal rate was increased significantly. In Figure 7, the spatial distribution of the 105 remaining $M_{0,w}$ estimates and their confidence interval is plotted in two cross sections, one parallel and one perpendicular to the series of pumping wells. As expected, the $M_{0,w}$ estimates are highest near the pumping wells; the left row of wells, which have deeper screens, causes stronger drawdowns than the right row. In the perpendicular cross section, the pattern of $M_{0,w}$ approximates the shape of a drawdown cone. The $M_{0,w}$ estimates at shallow well screens are clearly lower than at deeper well screens; this may be caused by a resistance layer or by recharge from ditches or creeks. This is in line with the head series of these observation wells (not shown here), where head differences between higher and lower screens range up to 4 m. Although the model fit is low in the vicinity of the pumping well screens (within a radius of about 200 to 300 m), all in all, the $M_{0,w}$ estimates seem nevertheless reasonable. The estimates of other parameters near the wells, however, are clearly biased. In Figure 8, cross sections are shown of R^2_{adj} and $M_{0,e}$ for the observation wells in the vicinity of the pumping wells. The low values of R^2_{adj} near the pumping well screens correlate with the low values of $M_{0,e}$. As it is not logical for the influence of evapotranspiration to be

Table 2
Range of Model Results and Parameter Estimates for All 139 Ground Water Head Series

Parameter	Minimum ($\pm 2\sigma$)	Median	Maximum ($\pm 2\sigma$)
R^2_{adj}	38.1	85.9	97.5
$M_{0,p}$	59 ($\pm 1.3 \times 10^3$)	864	6580 ($\pm 3.5 \times 10^5$)
$M_{0,\mathrm{e}}$	172 (± 122)	790	7976 (± 5913)
$M_{0,w}$	1.93×10^{-8} ($\pm 4.1 \times 10^{-5}$)	4.50×10^{-5}	1.25×10^{-2} (± 0.20)
f	0.09 (± 0.31)	1.20	4.29 (± 87)
d	-3.21	1.26	7.01

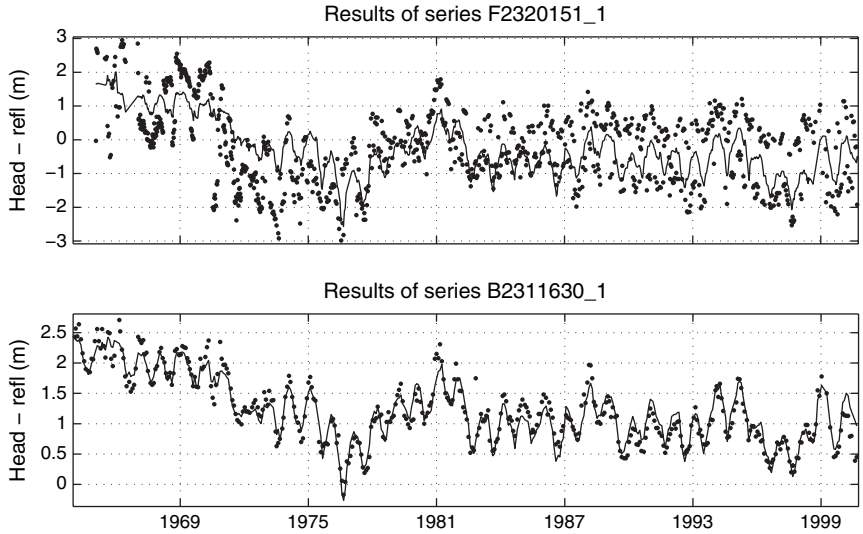

Figure 6. Head observations and predictions of wells F2320151 (near the pumping station) and B2311630 (at some distance), giving an indication of good and bad model fits.

heterogeneous in deeper soil layers, this indicates that the influence of evapotranspiration is overestimated and partly correlates with the effect of the individual pumping wells.

Discussion and Conclusions

In this paper, the PIRFICT model for time series analysis was extended to handle multiple inputs. For stresses other than areal recharge, analytical solutions of simple hydrogeological schematizations were used as a guide to develop appropriate impulse response functions. Different stresses are not necessarily connected in parallel in the model, as is the standard procedure in ARMA models. A case with a single observation well was used to illustrate how the model can effectively decompose head series into partial series that each show the effect of an individual stress. In the example with multiple observation wells, it was shown that, next to its a priori use in defining the impulse response functions, physical knowledge is also valuable in checking the consistency and plausibility of the model results a posteriori. The parameter values should fall within a range that is physically plausible. The spatiotemporal patterns observed in the variables supply important and independent feedback on the results, as there is no spatial dependency imposed on the models. By focusing on the model residuals, missing stresses, processes, or other sources of error may be readily identified. High error levels are a possible source of bias in the estimates, as other stresses may partly compensate missing stresses when their influence is correlated. In this case, the main source of error was the fact that the behavior of the individual pumping wells was not accounted for. In spite of this, the overall drawdown pattern of the wellfield in total, which is often the factor of interest, was represented well. The spatial distribution showed that the estimates for the evaporation series were clearly biased. Such a problem may be

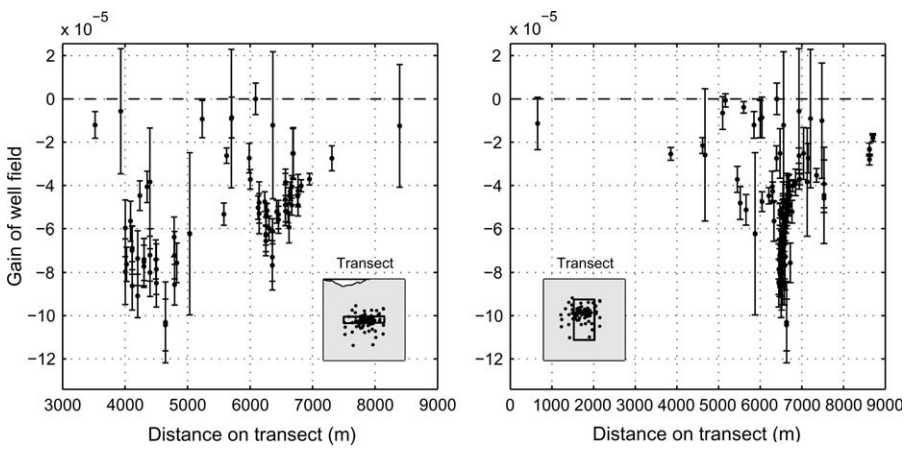

Figure 7. Estimated gains (dots) for the wellfield in the different observation wells presented in west-east (left) and north-south (right) cross sections. The error bars indicate the 95% confidence interval of the estimates.

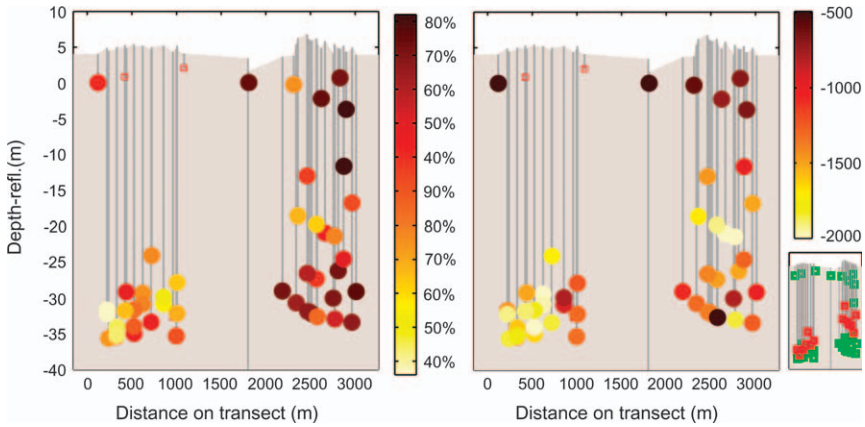

Figure 8. West-east cross sections near the pumping wells showing the percentage of variance accounted for (left) and the estimated gain of the evapotranspiration (right) in the different observation wells. The values of both are lowest near the pumping well screens (the red markers in the figure bottom right).

corrected by incorporating data on the missing factors in the model (in this case, the pumping at individual wells). If such data are not available (as in this case), the bias can be reduced by constraining the optimization problem to a realistic range based on the values and patterns in the surrounding observation wells. Future research will include methods to impose a spatial coherence a priori in the model, so that the individual dynamics of a high number of pumping wells can be incorporated in the model and the results of neighboring observation wells are linked and remain plausible.

The presented time series model may be applied to decompose series of head fluctuations into partial series, representing the influence of individual stresses. This enables the evaluation of individual effects of a stress, such as hydrological interventions, pumping wells, climatic changes, and surface water levels. Furthermore, the presented model may be used for forecasting, gap filling, scenario studies, trend analyses, and optimization and control of hydrogeological systems (using more or less standard time series analysis methods; e.g., Hipel and McLeod [1994]). The PIRFICT approach is particularly suited for the batch processing of many series, it uses a small number of parameters, and it is not limited by irregular or high-frequency data. Although here we specifically focus on ground water heads, the approach presented can also be applied to (contaminant) transport problems or for that matter to hydrological problems in general. In the field of transport, the Pearson III function has proven to be well usable also (it matches the convection-dispersion equation [e.g., Jury and Roth 1990; Maas 1994]), whereas in other fields, care has to be taken to select appropriate impulse response functions and methods for the processes and stresses occurring there.

An attractive feature of time series models is that they are based on relatively few assumptions and the fits are generally high; the model lets the data more or less speak for itself. As such, time series models are a valuable tool for preprocessing ground water level series before calibrating a ground water model. Using time series models, missing stresses or series that are influenced by hydrological interventions may be readily identified. Also, series may be identified that are not suitable for model calibration, for example, because they represent a hydrological feature that is not incorporated in the model, such as perched water tables. One step further, transient ground water models may be calibrated directly on the moments of the impulse response functions estimated with time series analysis (Van de Vliet and Boekelman 1998; Von Asmuth and Maas 2001), which requires the calibration of steady models only. Moments of the impulse response functions can also be modeled spatially with the analytic element method, creating a possibility for transient modeling with analytic elements (Bakker et al. 2007).

Acknowledgments

The authors wish to thank the Provincial Council of Limburg, the drinking water company OOWV and Kiwa Water Research for funding the research. We also thank Andrés Alcolea and two anonymous reviewers for their detailed and constructive comments, which helped to improve the paper.

References

Abramowitz, M., and I.A. Stegun. 1964. *Handbook of Mathematical Functions*. New York: Dover Publications Inc.

Bakker, M., K. Maas, F. Schaars, and J.R. Von Asmuth. 2007. Analytic modeling of groundwater dynamics with an approximate impulse response function for areal recharge. *Advances in Water Resources* 30, no. 3, doi: 10.1016/j.advwatres.2006.04.008: 493–504.

Box, G.E.P., and G.M. Jenkins. 1970. *Time Series Analysis: Forecasting and Control*. San Fransisco, California: Holden-Day.

Bruggeman, G.A. 1999. *Analytical Solutions of Geohydrological Problems*. Amsterdam, The Netherlands: Elsevier.

De Gooijer, J.G., B. Abraham, A. Gould, and L. Robinson. 1985. Methods for determining the order of an autoregressive-moving average process: A survey. *International Statistical Review* 53, no. 3: 301–329.

Hantush, M.S. 1956. Analysis of data from pumping tests in leaky aquifers. *Transactions, American Geophysical Union* 37, no. 6: 702–714.

Hipel, K.W., and A.I. McLeod. 1994. *Time Series Modelling of Water Resources and Environmental Systems*. Amsterdam, The Netherlands: Elsevier.

Jury, W.A., and K. Roth. 1990. *Transfer Functions and Solute Movement through Soil: Theory and Applications*. Basel, Switserland: Birkhäuser Verlag.

Knotters, M., and J.G. De Gooijer. 1999. Tarso modelling of water table depths. *Water Resources Research* 35, no. 3: 695–705.

Luo, J., O.A. Cirpka, and P.K. Kitanidis. 2006. Temporal-moment matching for truncated break-through curves for step or step-pulse injection. *Advances in Water Resources* 29, no. 9: 1306–1313.

Maas, C. 1994. On convolutional processes and dispersive groundwater flow. Ph.D. thesis, Delft University of Technology, Delft, The Netherlands.

Penman, H.L. 1948. Natural evaporation from open water, bare soil and grass. *Proceedings of the Royal Society of London* A193, no. 1032: 120–146.

Van de Vliet, R.N., and R. Boekelman. 1998. Areal coverage of the impulse response with the aid of time series analysis and the method of moments [in Dutch]. *Stromingen* 4, no. 1: 45–54.

Von Asmuth, J.R., and M.F.P. Bierkens. 2005. Modeling irregularly spaced residual series as a continuous stochastic process. *Water Resources Research* 41, no. 12: W12404, doi: 10.1029/2004WR003726.

Von Asmuth, J.R., and M. Knotters. 2004. Characterising spatial differences in groundwater dynamics based on a system identification approach. *Journal of Hydrology* 296, no. 1–4: 118–134.

Von Asmuth, J.R., and C. Maas. 2001. The method of impulse response moments: A new method integrating time series-, groundwater- and eco-hydrological modelling. *In Impact of Human Activity on Groundwater Dynamics*, ed. J.C. Gehrels, N.E. Peters, E. Hoehn, K. Jensen, C. Leibundgut, J. Griffioen, B. Webb, and W.J. Zaadnoordijk, 51–58. Publication no. 269. Wallingford, UK: IAHS.

Von Asmuth, J.R., M.F.P. Bierkens, and C. Maas. 2002. Transfer function noise modeling in continuous time using predefined impulse response functions. *Water Resources Research* 38, no. 12: 23-1–23-12.

Yu, C., A.W. Warrick, and M.H. Conklin. 1999. A moment method for analyzing breakthrough curves of step inputs. *Water Resources Research* 35, no. 11: 3567–3572.